Med & Health Jul 2026; 21(2): 1056-1079 https://doi.org/10.17576/MH.2026.2102.30

ORIGINAL ARTICLE

Tracking and Therapeutic Effects of a Single Dose Wharton's Jelly-derived Mesenchymal Stem Cell Intra-Articular Injection in a Guinea Pig Osteoarthritis Model Over 56 Days of Follow-up: A Pilot Study

BADRUL AKMAL HISHAM YUSOFF[1]*, AHMAD FARIHAN MOHD DON[1], NORLELAWATI MOHAMAD[1], RAMESH SARAVANAMUTHU[2], KARTHIK CHANDRAN[2,3], RAZIANA RASIB[2], PREMASANGERY KATHIVALOO[2,3], SU-YIN[1], SAREH KAMRAN[3]

[1]Department of Orthopedic & Traumatology, Faculty of Medicine, Universiti Kebangsaan Malaysia, 56000 Cheras, Kuala Lumpur, Malaysia

[2]Meluha Therapeutics Sdn Bhd, 62250 Precinct 10, Putrajaya, Malaysia

[3]Celler Therapeutics Sdn Bhd, 46300 Petaling Jaya, Selangor, Malaysia

**Correspondence: badortho@gmail.com; Tel: +6012 5196119*

Received: 05 November 2025 / Accepted: 12 Februari 2026

ABSTRAK

Osteoartritis (OA) merupakan beban kesihatan global yang utama, menjejaskan lebih daripada 600 juta orang di seluruh dunia pada tahun 2021 dan jumlah ini dijangka terus meningkat dalam beberapa dekad akan datang. Terapi sel stem mesenkimal kini sedang dikaji sebagai pilihan rawatan untuk OA lutut. Kajian ini bertujuan untuk menilai keberlangsungan dan kesan terapeutik sel stem mesenkimal yang diperoleh daripada jeli Wharton manusia (WJ-MSC) selepas satu suntikan intra-artikular (1.7×10^7 sel/kg) dalam model OA 'guinea pig', menggunakan enam ekor haiwan dalam kumpulan rawatan WJ-MSC dan empat dalam kumpulan kawalan. Hasil utama kajian ialah ketebalan rawan, skor degenerasi rawan mengikut 'Osteoarthritis Research Society International' (OARSI), serta keberlangsungan WJ-MSC. Dalam kajian ini, WJ-MSC berlabel PKH26 disuntik ke dalam lutut kanan dan dijejaki pada hari 0, 7, 14, 28 dan 56. Lutut haiwan dikumpulkan pada hari ke-56 untuk penilaian makroskopik, skor OARSI serta analisis histologi menggunakan pewarnaan Hematoxylin & Eosin dan Safranin O. Hasil kajian menunjukkan bahwa WJ-MSC kekal hidup sehingga 56 hari. Sendi yang dirawat menunjukkan pengurangan keterukan OA, dengan peningkatan ketebalan rawan sebanyak 108% pada kondil femur medial ($p = 0.002$), 36% pada kondil femur lateral, 47% pada plat tibia medial ($p = 0.02$*) dan 45% pada plat tibia lateral berbanding kawalan. Tiada tanda-tanda keganasan diperhatikan. Secara keseluruhan, suntikan dos tunggal WJ-MSC memberikan bukti konsep yang menyokong pelaksanaan kajian lebih mendalam pada masa hadapan.*

Kata kunci: *Guinea pig; ketebalan rawan; osteoartritis lutut; suntikan intra-artikular; WJ-MSCs*

ABSTRACT

Osteoarthritis (OA) is a major global health burden, affecting over 600 million people worldwide as of 2021, with numbers projected to rise significantly in the coming decades. Mesenchymal stem cell therapy is currently being investigated as a treatment option for knee OA. This study aimed to evaluate the persistence and therapeutic effects of human Wharton's Jelly-derived mesenchymal stem cells (WJ-MSCs) following a single intra-articular injection (1.7×10^7 WJ-MSC cells/kg) in a guinea pig OA model, using six animals in the WJ-MSC treatment group and four animals in the control group. The

primary endpoints are cartilage thickness, Osteoarthritis Research Society International (OARSI) cartilage degeneration scores measurements and persistence of WJ-MSCs. In this experiment, PKH26-labeled WJ-MSCs were injected into the right knee and tracked on days 0, 7, 14, 28 and 56. Knees were harvested on day 56 for macroscopic assessments, OARSI cartilage scoring, and histology using haematoxylin and eosin, and Safranin O staining. As a result, the WJ-MSCs remained persistent for up to 56 days. WJ-MSC-treated joints showed reduced OA severity, with increased cartilage thickness of 108% at the medial femur condyle ($p = 0.002$*), 36% at the lateral femoral condyle, 47% at the medial tibia plateau ($p = 0.02$*) and 45% at the lateral tibia plateau compared with controls. No signs of malignancy were observed. Overall, a single dose injection of WJ-MSC provided a proof-of-concept to conduct further research in the future.

Keywords: Cartilage thickness; guinea pig; intra-articular injection; knee osteoarthritis; WJ-MSCs

INTRODUCTION

Osteoarthritis (OA) is the most common type of arthritis and a degenerative joint disease. The earliest changes associated with OA are in articular cartilage, including surface fibrillation, in which the cartilage loses its smooth shape, texture and focal erosion, which leads to cartilage degradation (Sen & Hurley 2023). Globally, an estimated 595 million people were diagnosed with OA in 2020, which is equal to 7.6% of the global population, and an increase of 132.2% in total cases since 1990. Compared with 2020, cases of OA are projected to increase by 74.9% for knee OA by 2050 (Steinmetz et al. 2023). Another study revealed that OA is indeed a major global health burden, affecting over 600 million people worldwide as of 2021, with numbers projected to rise significantly in the coming decades. It is a leading cause of disability, causing pain and functional impairment and imposes substantial socio-economic costs, including healthcare expenses and loss of productivity. OA prevalence and incidence are increasing globally, particularly with aging populations and in regions with higher socio-economic development. This growing prevalence poses significant challenges to healthcare systems and necessitates urgent public health strategies to increase awareness, early diagnosis, treatment and prevention efforts worldwide (Luo et al. 2025).

Moreover, East and Southeast Asia are experiencing marked increases in OA incidence, prevalence and disability, driven by population ageing, rising obesity and high physical occupational demands. Southeast Asia shows the fastest growth in new OA cases, while East Asia has the steepest rise in prevalence and OA-related disability. These trends place substantial pressure on public health systems and underscore the need for earlier diagnosis and updated clinical management strategies (Zhou et al. 2025).

Risk factors linked to the development of OA include ageing, female sex, obesity or overweight, history of joint injury, sports, and activities that place heavy loads on joints (Schram et al. 2020). These risk factors are known to accelerate cartilage matrix loss, increase cartilage fibrillation and promote subchondral bone changes (Goldring 2012), features that are reflected in the key parameters assessed in this study. Current OA management options include nonsteroidal anti-inflammatory drugs (NSAIDs), opioid analgesics, intra-articular injections of steroids and hyaluronic acids, and surgery (Jiang et al. 2024). However, these approaches are directed toward pain management rather than cartilage regeneration or the inhibition of inflammation. Since articular cartilage does not heal with conventional therapy, its regeneration is an important therapeutic approach for the treatment of OA (Harrell et al. 2019).

In recent years, mesenchymal stem cells (MSCs) have attracted attention as a promising therapeutic agent for cartilage restoration and regeneration. This is due to their unique ability to differentiate into different cell types, including

chondrocytes, which are necessary for cartilage regeneration. MSCs can be derived from bone marrow, adipose tissue and umbilical cord. The unique features of these cells, such as their ability for self-renewal and multipotency, make them ideal regenerative therapeutic agents in defective cartilage. In addition, MSCs exert immunomodulatory and anti-inflammatory paracrine effects, thereby reducing inflammation and supporting tissue repair in OA. Therefore, scientists claim that MSC-based therapy addresses the root cause of OA by offering cartilage tissue regeneration, improving joint function and suppressing disease progression (Wu et al. 2024). Moreover, Wharton's Jelly-derived mesenchymal stem cells (WJ-MSCs) have a secretome that contains a rich profile of growth factors, cytokines and extracellular vesicles that collectively create a pro-regenerative joint environment. Key factors such as transforming growth factor-beta (TGF-β), insulin-like growth factor-1 (IGF-1) and fibroblast growth factor-2 (FGF-2) enhance chondrocyte survival, stimulate matrix synthesis and promote the regeneration of cartilage. Anti-inflammatory cytokines, including interleukin-10 (IL-10) and tumour necrosis factor-alpha-stimulated gene/ protein-6 (TSG-6), suppress synovial inflammation and reduce catabolic pathways driven by nuclear factor kappa-light-chain-enhancer of activated B cells (NF-κB) and inflammatory mediators, thereby slowing cartilage breakdown. WJ-MSCs also release vascular endothelial growth factor (VEGF) and hepatocyte growth factor (HGF), which support subchondral bone and vascular homeostasis, while antioxidant molecules released by these cells help mitigate oxidative stress in the OA joint. Their extracellular vesicles and exosomes deliver chondroprotective microRNAs that inhibit chondrocyte apoptosis, reduce matrix metalloproteinase (MMP) expression and enhance collagen production. Through these combined paracrine actions, WJ-MSCs modulate the inflammatory microenvironment, protect existing cartilage from degradation and promote structural repair (Barlian et al. 2020). Therefore, WJ-MSCs were used in this study among other sources.

Despite increasing interest in intra-articular MSC therapy for knee OA, a key unresolved issue is the lack of in-vivo evidence linking WJ-MSCs cell persistence within the joint to sustained structural cartilage benefit following a single, and possibly clinically relevant dose. This may leave some uncertainty as to whether MSCs remain in the osteoarthritic joint long enough to exert a meaningful effect. This gap could make it difficult to come up with a rational dose selection. Therefore, the present study was designed primarily to track human WJ-MSCs following a single intra-articular injection in a guinea pig OA model and to evaluate their persistence alongside cartilage thickness and OARSI score, over a 56-day follow-up period.

However, using cell therapy is associated with several clinical translation challenges related to cell heterogeneity, uncertain dosing, and regulatory and manufacturing limitations (Česnik & Švajger 2024). MSCs are inherently heterogeneous, and their characteristics can vary widely depending on donor age, tissue source, isolation method, culture condition and regenerative potential, complicating efforts to reproduce consistent therapeutic effects across patients or trials (Česnik & Švajger 2024).

In addition, dosing and administration protocols remain major obstacles. Clinical trials in OA and other conditions have used greatly varying cell numbers, injection volumes, frequencies and delivery routes. This makes it difficult to define a universal therapeutic dose. Moreover, the survival, retention and functional activity of MSCs, especially when injected into an inflamed or degenerated joint environment, remain uncertain. Without standardised, evidence-based dosing regimens and robust data on cell persistence, it is challenging to predict safety, durability and efficacy in patients (Mello et al. 2024).

Finally, regulatory and manufacturing issues pose a significant barrier to clinical translation. MSC-based products are often categorised as advanced therapy medicinal products (ATMPs), requiring compliance with Good Manufacturing

Practice (GMP) standards. The lack of a globally harmonised regulatory framework for defining what constitutes an MSC product, what potency metrics should be used, and how products should be standardised, complicates regulatory approval and commercialisation (Crescencia 2024). These challenges suggest that while MSC-based therapies show strong preclinical promise, significant work remains before they can reliably translate into safe, effective and widely available clinical treatment; therefore, the present study should be regarded as a proof of concept, and further studies are required to address regulatory, manufacturing and standardisation requirements.

Among all stem cells, WJ-MSCs are widely used in OA treatment compared to other MSC sources because they possess a unique combination of high regenerative capacity, strong chondrogenic differentiation potential, and potent immunomodulatory and anti-inflammatory properties, which are essential for cartilage repair and inflammation reduction in OA (Ghamrawi et al. 2025).

A review study revealed that WJ-MSCs are superior to other MSC sources because they reduce the risk of immune rejection due to their lower immunogenicity; they also show higher proliferation capacity, delayed senescence and have an enriched profile containing potent immunomodulatory, anti-inflammatory angiogenic and regenerative factors. Additionally, WJ-MSCs are obtained through a non-invasive, ethically uncomplicated process from umbilical cord tissue (Watson et al. 2015), making them safer and more practical for therapeutic applications compared with adult MSCs (Drobiova et al. 2023). Furthermore, WJ-MSCs exert paracrine activity through the secretion of various growth factors and signal-transmitting molecules that support tissue regeneration (Liang et al. 2020).

To support the use of WJ-MSCs for OA, several pre-clinical studies have demonstrated their potential to relieve pain, protect joint tissue and promote cartilage regeneration (Aratikatla et al. 2024; Endrinaldi et al. 2019a; Endrinaldi et al. 2019b; Zhang et al. 2021). Despite the abundance of pre-clinical studies supporting the safety and efficacy of MSCs for OA treatment, ongoing pre-clinical research remains important due to several unsolved scientific, technical and translational challenges. These include optimising MSC sources (Mastrolia et al. 2019), delivery methods (Zhou et al. 2021), cell viability and ensuring consistent therapeutic outcomes (Wu et al. 2024). In line with this, the primary aim of this study is to assess the duration of WJ-MSCs persistence and efficacy of a single intra-articular injection of these cells in treating OA using a xenographic Dunkin Hartley guinea pig model.

While the current study was not designed to directly optimise MSC sources, delivery methods or manufacturing-related variables, it addresses a complementary and necessary preclinical gap by evaluating in-vivo cell persistence and histological outcomes. By demonstrating WJ-MSC persistence and cartilage-protective effects without adverse findings, this work provides foundational evidence to support future targeted studies aimed at addressing these broader translational challenges.

The Dunkin Hartley guinea pig is widely recognised as one of the most translationally relevant rodent models for human knee osteoarthritis because it develops spontaneous, primary OA with a natural onset, disease progression and joint pathology that closely resemble human ageing-related OA. This strain shows progressive cartilage degeneration, mobility decline and inflammation that mirror human musculoskeletal aging. These characteristics make the Dunkin Hartley model highly suitable for evaluating regenerative therapies and for preclinical studies aimed at human translation (Musci et al. 2020).

The therapeutic outcomes expected in this study were focused on assessing whether WJ-MSC administration could attenuate OA-related knee degeneration. Specifically, we aimed to determine whether intra-articular injection of WJ-MSCs could improve cartilage integrity as reflected by increased cartilage thickness, lower OARSI score compared to the control group and create more favourable histological features. In addition, because safety is important,

we evaluated the short-term persistence of the injected cells, the absence of abnormal tissue formation and the lack of malignancy via observations. Together, these outcomes were selected to provide evidence of both the regenerative potential and safety profile of WJ-MSCs in this animal model to support the proof-of-concept.

MATERIALS AND METHODS

Study Design

This preclinical study aimed to assess the efficacy of human-derived WJ-MSC in treating knee OA in Dunkin Hartley guinea pigs. A total of ten male animals (700 g, age 4-5 months) were used, where six guinea pigs in the WJ-MSC treatment group were injected intra-articularly with a single dose of human WJ-MSC (1.7×10^7 WJ-MSC cells/kg), and four guinea pigs in the control group remained untreated. In this study, animals in the WJ-MSC and control group were age- and weight-matched male Dunkin Hartley guinea pigs, a strain known to develop spontaneous OA by 4-5 months of age, at which stage OA was established but had not yet progressed to advanced disease (Musci et al. 2020). No separate pre-treatment OA grading was performed prior to intervention; instead, the untreated OA control group was used to represent the baseline OA status at the same age and disease stage. Because both groups were comparable in age, body weight and housing conditions, differences observed between the WJ-MSC-treated and control groups were considered to be attributed to the treatment effect rather than baseline variability.

A sham-injection group was not included because it would require additional needle penetration and joint manipulation without providing therapeutic benefit, which conflicted with the 3Rs principle of refinement. Ethical analyses of sham procedures in research had shown that such interventions can expose subjects to procedural risk, pain or harm, which at this point may not add meaningful scientific value (Resnik & Miller 2010). Primarily, in-vivo imaging was conducted to determine the duration of the WJ-MSC remaining in the knee post-intra-articular injection, and the efficacy and safety of the WJ-MSC in the knee OA were examined through histopathological examination.

Wharton's Jelly-derived Mesenchymal Stem cells Preparation

WJ-MSCs were prepared and characterised for this study at a National Pharmaceutical Regulatory Agency (NPRA) Grade A laboratory facility in Putrajaya, Malaysia, operated by a Meluha Life Sciences Sdn Bhd subsidiary. The preparation was conducted in a GMP-compliant laboratory certified by the International Organisation for Standardisation (ISO) 14644-1:1999E and following the guidelines for Cellular and Gene Therapy Products and Good Tissue Practice (GTP).

The WJ-MSCs were obtained from umbilical cords of full-term human placentas by elective cesarean section after informed consent from healthy donors and were aseptically stored in sterile phosphate-buffered saline (PBS) (Sigma-Aldrich, P4739, St. Louis, Missouri, USA) supplemented with 1% Penicillin–Streptomycin (Pen/Strep) antibiotics. The umbilical cord blood was sent for human immunodeficiency virus (HIV), Hepatitis B and C, Cytomegalovirus (CMV) and syphilis screening. The umbilical cord was sectioned into smaller pieces (approximately 2 cm per piece), the blood vessels were removed, and digested with collagenase (Merk, 1148089, Darmstadt, Germany) to break down the extracellular matrix overnight. The collagenase was then neutralised by Complete Culture Media (CCM) [Gibco (Thermo Fisher Scientific, USA)], and the cords were then transferred into a sterile T-flask (Corning, CLS431082, NY, USA) and incubated for seven days (Varaa et al. 2019).

The CCM included KnockOut Dulbecco's Modified Eagle Medium (DMEM) (Gibco, Thermo Fisher, New York, USA) supplemented with 1.25 % Human Serum AB Plasma (Sigma, H4522, St. Louis, Missouri, USA), 1% GlutaMAX supplement (Gibco, Thermo Fisher, 35050061,

New York, USA) and gentamicin (50 mg/ml) (Gibco, Thermo Fisher, 15750060, Waltham, Massachusetts, USA) at a final concentration of 1ml/L of CCM. Additionally, human recombinant basic fibroblast growth factor (bFGF) (50 µg/ml; StemCell Technologies, 15614959, Vancouver, BC, Canada) was added at 80 µL/L of CCM (Md Yusoff et al. 2023).

Wharton's Jelly-derived Mesenchymal Stem Cells Characterisation using Flow Cytometry

To confirm the identity and purity of the WJ-MSCs, flow cytometry was used to analyse the expression of specific surface markers. For this purpose, WJ-MSCs culture was monitored every 48 hours until they showed 80-90% confluency as an optimal growth rate. The WJ-MSCs were grown using a monolayer construct to maintain consistent expansion. An expected yield of 15 x 10^6 WJ-MSCs was obtained after seven days of incubation. The cells were then harvested, sub-cultured, and incubated for another seven days to induce further growth. At passage three, the WJ-MSCs were characterised according to the International Society for Cellular Therapy (ISCT), which involved an analysis of WJ-MSC-specific markers, including CD34, HLA DR, CD73 and CD90 using flow cytometry, BD FACSDiva analysis software (BD Biosciences, San Jose, USA) (Md Yusoff et al. 2023). Characterised cells were harvested and cryopreserved in a liquid nitrogen storage tank at -190°C for future use (Nadeem et al. 2024).

Trilineage Differentiation Assay

WJ-MSCs were seeded in 6-well plates and cultured to 70-80% confluence before being induced for lineage-specific differentiation using STEMPRO differentiation media (Thermo Fisher Scientific). For adipogenesis, cells were cultured in adipogenic induction medium for 21 days, followed by fixation and staining with Oil Red O (Abcam, 150678, Cambridge, United Kingdom) to detect lipid droplets. For chondrogenesis, cells were treated with chondrogenic medium for 21 days, fixed and stained with Alcian Blue (Sigma-Aldrich, B8438, Darmstadt, Germany) to visualise glycosaminoglycans in the cartilage matrix. For osteogenesis, cells were cultured in osteogenic induction medium (Sigma-Aldrich, C-28013, Heidelberg, Germany) for 21 days and stained with Alizarin Red S (Sigma-Aldrich, TMS-008, St. Louis, Missouri, United States) to detect calcium mineralisation. Control groups were maintained in standard growth medium without induction. All images were captured at 4x magnification using an inverted phase-contrast microscope (OLYMPUS) (Mallis et al. 2020).

Labelling of Wharton's Jelly-derived Mesenchymal Stem Cells with PHK26 to Enable In-vivo Tracking of the Administered Cells

Labeling WJ-MSCs with PKH26 allowed for in-vivo tracking of the administered cells by enabling their visualisation and localisation in tissues after transplantation; therefore, in this study, PKH26 fluorescent dye (Sigma Aldrich, PKH26GL, St. Louis, Missouri, USA) was used to track WJ-MSCs after administration in guinea pigs (Li et al. 2012). WJ-MSCs were labelled with PKH26 according to the standard protocol (Sigma Aldrich). Briefly, cells were labelled with PKH26 dye by first washing and resuspending them in serum-free media (centrifuged at 400x g for 5 minutes). The cell suspension was mixed with an equal volume of PKH26 dye, followed by 2 to 5 minutes of incubation at room temperature to allow dye incorporation into the cell membrane. The staining reaction was then stopped by adding an equal volume of serum, followed by incubation for 1 minute. Next, cells were washed several times to remove excess dye, centrifuged and resuspended before the labelled cells were ready for in-vivo tracking.

Dosage of Wharton's Jelly-derived mesenchymal stem cells Intra-articular Injection in Animals

In this study, a low dose (0.8 x 10^7 cells/ml),

medium dose (1.6 x 10^7 cells/ml) and high dose (2.4 x 10^7 cells/ml) of PKH26-labelled WJ-MSCs were selected. This selection was based on another study that determined a maximum tolerated dose (MTD) of greater than 2 x 10^7 cells/kg in guinea pigs with no toxic reactions or death observed (Cheng et al. 2024). Table 1 summarised the doses used in this experiment in cells/mL and cells/kg.

In this study, a volume of 0.5 mL of cell suspension in normal saline containing three doses of cells was injected into guinea pigs with an average body weight of 700 g:

$$\text{Injection volume per kg} = \frac{0.5 \text{ ml}}{0.7 \text{ kg}} = 0.714 \text{ ml/kg}$$

This preliminary trial was conducted to validate the success of PKH26 labelling of WJ-MSCs and assess their compatibility with the IVIS Lumina III imaging (PerkinElmer, Hopkinton, USA). The three selected doses underwent IVIS Lumina III imaging, and the high dose of WJ-MSCs (1.7 × 10^7 WJ-MSC cells/kg) showed the strongest signal. Therefore, the high dose of WJ-MSC was chosen as the only dose for the intra-articular injection in this study.

Xenograft Dunkin Hartley Guinea Pig Model

Ten male Dunkin Hartley guinea pigs (average body weight of 700 g) were obtained from Universiti Kebangsaan Malaysia (UKM) Laboratory Animal Research Unit. The guinea pigs were kept in individual cages in the animal house. The animal ethics for this study were approved by the UKM Medical Research Committee (FF-2019-450) and UKM Animal Ethics Committee (PPUKM/2019/BADRUL AKMAL/25-SEPT/1038-OCT-2019-MARCH-2020) on 24 October 2019. Moreover, the Guideline for the Housing of Guinea Pigs in Scientific Institutions was followed in this experiment (Animal Research Review Panel 2023). The guinea pigs were checked for diseases like skin disease and gum ulcers before the commencement of the study. The animals had access to water freely and were fed daily with guinea pig pellets, hay, fresh vegetables and fruits.

TABLE 1: Experimental doses were reported as cells/mL and their equivalent measurement as cells/kg. All three doses did not exceed the MTD dose (2 × 10^7 cells/kg).

Dose (cells/mL)	Dose (cells/kg)
Low dose: 0.8 x 10^7 cells/ml	0.8 × 10^7 × 0.714 = 5.7 × 10^6 cells/kg
Medium dose: 1.6 x 10^7 cells/ml	1.6 × 10^7 × 0.714 = 1.1 × 10^7 cells/kg
High dose: 2.4 x 10^7 cells/ml	2.4 × 10^7 × 0.714 = 1.7 × 10^7 cells/kg
MTD: Maximum tolerated dose	

Intra-articular Injection of Wharton's Jelly-derived Mesenchymal Stem Cells

Knee intra-articular injection was performed on the guinea pigs under anaesthesia. All injections were performed by the same surgeon to ensure consistency of technique. To sedate animals for 30-45 minutes, an anaesthetic mixture of ketamine, zoletil and xylazine (KTX) was administered intramuscularly at a volume of 0.2 mL/kg (Wellington et al. 2013). The injection was given into the right hind thigh muscle (Horie et al. 2012), using an insulin syringe (31G × 5/16", 1 mL). For the WJ-MSC treatment group, 1.7 × 10^7 WJ-MSC (cells/kg) suspended in 0.5 mL normal saline were injected into the lateral compartment

of the right hind knee. A 21-gauge needle was used for this intra-articular injection, inserted just behind the lateral edge of the patellar ligament and directed through the triangle formed by the femoral epicondyle, tibial plateau and the notch where they meet. The same injection procedure was used for the control group, but instead of cells, 0.5 mL of normal saline was administered.

In-vivo Tracking of the Cells

Imaging was performed on the guinea pigs under anaesthesia as mentioned in the previous paragraph. The WJ-MSC-treated group underwent imaging procedures on days 0, 7, 14, 28 and 56 for in-vivo tracking of the WJ-MSCs (Goto et al. 2021; Shin et al. 2022). The in-vivo tracking of WJ-MSCs was done using Perkin Elmer IVIS Lumina III (Caliper Life Sciences, Hopkinton, Massachusetts, USA), capable of fluorescent imaging reporters with the following settings: excitation at 535 nm and emission at 580 nm (PKH26 filter set), exposure time of 1 to 5 seconds depending in signal intensity, field of view set to 12.5 cm, binning at medium, f/stop = 1, and automatic background subtraction was enabled. After sedating the guinea pig, the animals were placed prone in the IVIS Lumina III chamber, and images were captured. The serial images captured by the IVIS Lumina III determined the duration for which the WJ-MSCs remain in the knee joint. The lesser the signal detected, the fewer the WJ-MSCs. The imaging procedure was stopped on day 56 as no more fluorescent signals were detected.

Macroscopic Examination of The Knee

All 10 guinea pigs were euthanised for macroscopic examination on day 56, according to the UKM Animal Ethics Committee euthanasia guidelines (UKM Animal Ethical Committee 2025), which encouraged intracardiac pentobarbitol (Dechra, NDC 17033-085-25) 200 mg injection. Fur over the right hind knee was shaved, the right hind knee was harvested, and an arthrotomy for the right hind knee was done to expose the distal femur condyle and tibial plateau. The medial and lateral meniscus was removed to get a complete view of the tibial plateau. The joint surface was washed with normal saline, and the cartilage surface was examined macroscopically. Each cartilage surface was given a score, and the total score for each knee was calculated using the Osteoarthritis Research Society International (OARSI) cartilage score (Waldstein et al. 2016).

Osteoarthritis Research Society International Cartilage Scoring

The cartilage was graded using the OARSI cartilage scoring for osteoarthritis in guinea pigs (Table 2) (Waldstein et al. 2016). The knee joint score was calculated based on the changes at the femur condyle and tibia plateau by multiplying the cartilage grade by the area of the lesion. The higher the joint score, the more severe the OA. This scoring was performed by an independent evaluator who was blinded to the treatment groups to minimise observer bias. Table 2 showed OARSI cartilage scoring for osteoarthritis in guinea pigs.

TABLE 2: OARSI cartilage scoring for osteoarthritis in guinea pigs

Parameter	Grade
Normal	0
Fissures into superficial zone (fibrillation)	1
Erosion into superficial or middle zones	2
Erosion into deep zone	3
Erosion full depth (bone exposed)	4

OARSI: The Osteoarthritis Research Society International

Histological Examination and Cartilage Thickness Measurement

All the harvested hind knees were fixed in 10% buffered formaldehyde solution. The knee specimens were cut into 5 x 20 mm and placed into histology cassettes for grossing. Since the tissue is a calcified specimen, decalcification was required before processing the tissue. The tissue was decalcified by soaking overnight in Osteosoft solution (Merck KGaA, Darmstadt, Germany). The tissue was processed using Revos Tissue Processor by Thermo Fisher Scientific (Waltham, MA, USA). The tissue was then clamped on a microtome. Microtomy was done using a Leica RM2245 microtome to obtain tissues of 3 µm thickness. Eventually, the specimens were mounted on glass slides (Xu et al. 2024).

Upon tissue processing, the tissues were stained with haematoxylin and eosin to look at the structural integrity of the tissue and Safranin O stain to detect cartilage thickness using the standard protocol. The cartilage thickness was measured at the centre of each femur condyle and tibia plateau from the superficial surface of the cartilage to the calcified-noncalcified tidemark (Nadeem et al. 2024).

Statistical Analysis

In this study, descriptive statistics and normality tests were performed using the Explore function in Statistical Package for the Social Science. version 29 (IBM Corp, Armonk, NY, USA) to evaluate the distribution of the data. Given the unequal group sizes and variability, Welch's t-test (equal variances not assumed) was applied for independent group comparisons, with statistical significance set at $p < 0.05$ (Kent State University Libraries 2025). Confidence intervals of 95% were calculated for the body weight and cartilage thickness measurements using Microsoft Excel (Microsoft Corporation, Redmond, WA) to provide an estimate of the precision and variability around the observed mean differences. Effect size was calculated directly in SPSS using Hedges' g values for cartilage thickness, which applied a small-sample correction and was therefore appropriate for the current sample size (n = 6 in the WJ-MSC group vs n = 4 in the control group).

Animals were randomly assigned to a treatment and a control group. All outcome assessments were performed by an investigator who was blinded to group allocation. Tissue samples were coded by an independent researcher before histological processing, ensuring that the scorer had no access to treatment information during analysis.

RESULTS

Mesenchymal Stem Cells' Morphology and Characterisation

To confirm the morphology of WJ-MSCs at passage three, a light microscope (Leica ICC50) was used, and the spindle shape of the cells was captured as shown in Figure 1A. After the cells reached 80% confluency within a week, characterisation of WJ-MSCs was performed by assessing a positive and negative panel of markers based on the ISCT guidelines using the flow cytometry technique. Flow cytometric analysis confirmed that an insignificant population of cells (<5%) expressed the negative markers, including CD34 and HLA DR, while more than 95% of the population expressed the positive markers, including CD73 and CD90. Figure 1B showed the flow cytometry analysis of protein expression on a bar chart and Figure 1C showed the flow cytometry histogram of this analysis. The results confirmed the presence of MSCs at a high percentage in the cell culture.

Trilineage Differentiation

WJ-MSCs demonstrated successful trilineage differentiation when cultured under specific induction conditions. Adipogenic differentiation was evidenced by the formation of intracellular lipid droplets stained red with Oil Red O, while chondrogenic differentiation resulted in an extracellular matrix rich in glycosaminoglycans, stained blue with Alcian Blue. Osteogenic

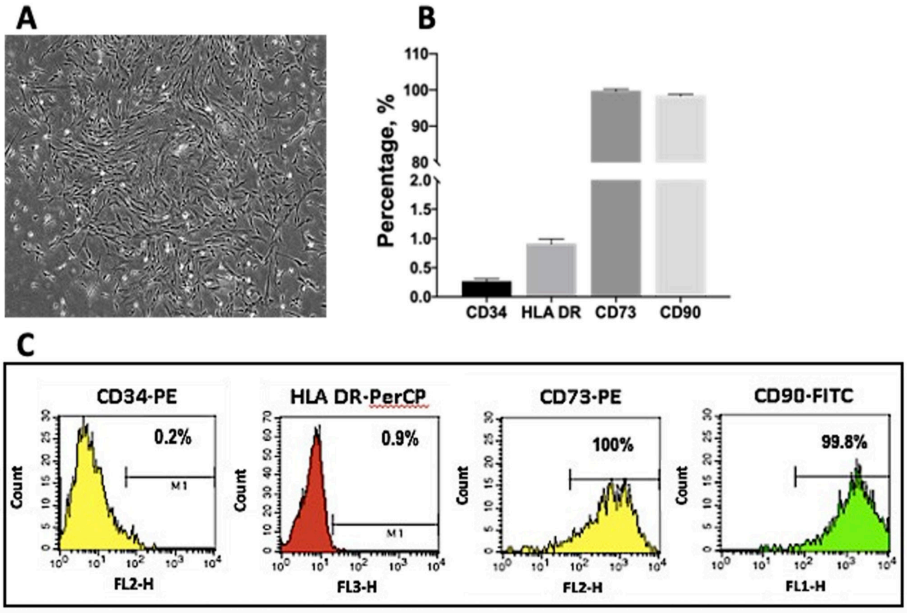

FIGURE 1: Morphology and characterisation of WJ-MSCs. (A) The morphology of MSCs in seven days of culture at passage three under a light microscope represents spindle-shaped cells; (B) Quantification of flow cytometry expression analysis of negative (CD34: 0.2%, HLA DR: 0.9%) and positive (CD73: 100%, CD90: 99.8%) cell surface markers represented on a bar chart; (C) Flow cytometry histogram plots represented negative and positive marker expression in WJ-MSC culture

differentiation was confirmed by the presence of mineralised calcium nodules stained red with Alizarin Red S. The control groups, maintained in standard growth medium, showed no lineage-specific staining. These findings confirmed the multipotent capacity of WJ-MSCs, as illustrated in Figure 2.

General Health of the Guinea Pigs

To ensure safety, monitor adverse effects and assess the tolerability of the treatment, the general health of the guinea pigs was observed. The guinea pigs were generally healthy post-intra-articular WJ-MSCs injection. The guinea pigs did not show any side effects like local inflammation, joint effusion, ulcers, poor appetite or reduction in movement. On average, the WJ-MSC-treated group showed significant weight gain compared to the control group at days 28 and 56 (Figure 3). Throughout the examination of the guinea pigs for 56 days, the WJ-MSC group had more frequent movements in their respective cages compared to the control group. Figure 3 showed the average body weight in each group, standard deviation (SD) and confidence interval (CI).

In-vivo tracking of Wharton's Jelly-derived Mesenchymal Stem Cells in the Knee using the IVIS Lumina III Imaging System

To track the presence and elimination of WJ-MSCs in the knees, the in-vivo imaging was done at day 0, 1, 7, 14, 28 and 56 days after intra-articular injection of WJ-MSCs labelled with PKH26 fluorescent dye using IVIS Lumina III imaging system. On day 0, before knee intra-articular injection (Figure 4A), no fluorescent signal was detected. Following knee intra-articular injection with WJ-MSCs on day 0, a

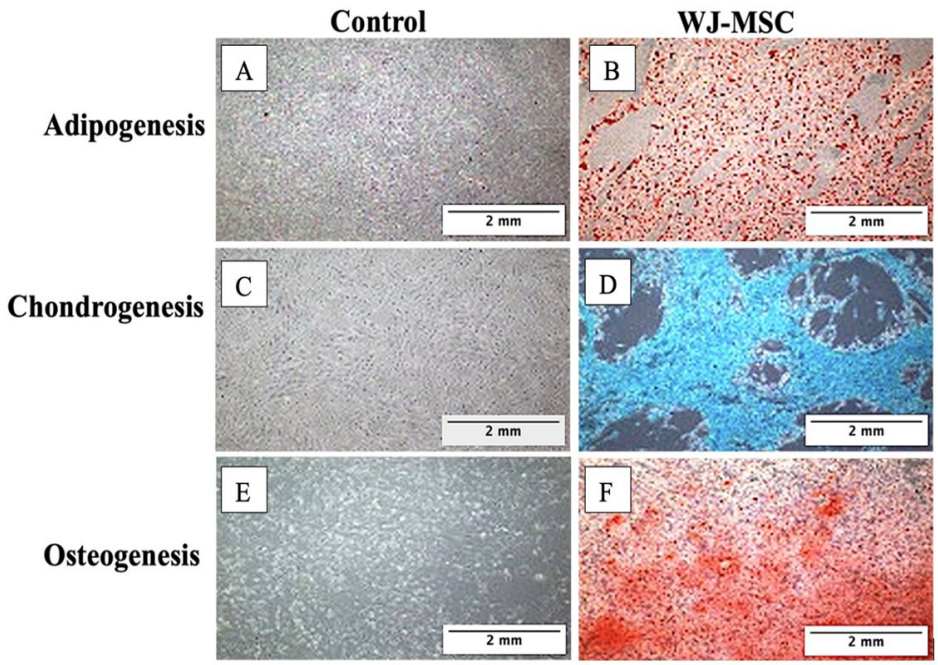

FIGURE 2: Trilineage differentiation potential of Wharton's jelly-derived mesenchymal stem cells (WJ-MSCs). (A) Control (undifferentiated WJ-MSCs) for adipogenesis, showing no Oil Red O staining; (B) Adipogenic differentiation of WJ-MSCs, showing positive Oil Red O staining (red) indicating intracellular lipid droplet formation; (C) Control (undifferentiated WJ-MSCs) for chondrogenesis, showing no Alcian Blue staining; (D) Chondrogenic differentiation of WJ-MSCs, showing positive Alcian Blue staining (blue) indicating proteoglycan-rich extracellular matrix formation; (E) Control (undifferentiated WJ-MSCs) for osteogenesis, showing no Alizarin Red S staining; (F) Osteogenic differentiation of WJ-MSCs, showing positive Alizarin Red S staining (red-orange) indicating calcium deposition and mineralized matrix formation. Cells were observed at 4x magnification using an inverted microscope. Scale bar: 2 m

high-intensity fluorescent signal was detected on the right hind knee (Figure 4B). On day 7 (Figure 4C), there was a fluorescent signal from the bilateral knee and caudal region of the guinea pig's body, which could correspond to the guinea pig's spine. On days 14 and 28 (Figure 4D and 4E), the signal pattern was similar to that on day 7, but the intensity gradually decreased. Imaging at day 42 was missed because of the movement control order due to COVID-19. Imaging of the guinea pigs resumed at day 56 (Figure 4F), and no more fluorescent signals were detected during the imaging procedure. We assumed the injected WJ-MSCs had been eliminated from the guinea pig body by day 56. From the serial in-vivo imaging, WJ-MSCs were concentrated on the bilateral knees and the lower spinal region of the guinea pigs. WJ-MSCs may have extruded from the small guinea pig knee during intra-articular inoculation.

Macroscopic Examination of the Knee

To examine the integrity of cartilage in treated and control groups, macroscopic examination was conducted. The observations of the WJ-MSC-treated guinea pigs revealed smooth cartilage surfaces on the femoral condyle and tibial plateau, with only minimal fibrillation observed (Figure 5A). In contrast, the control group

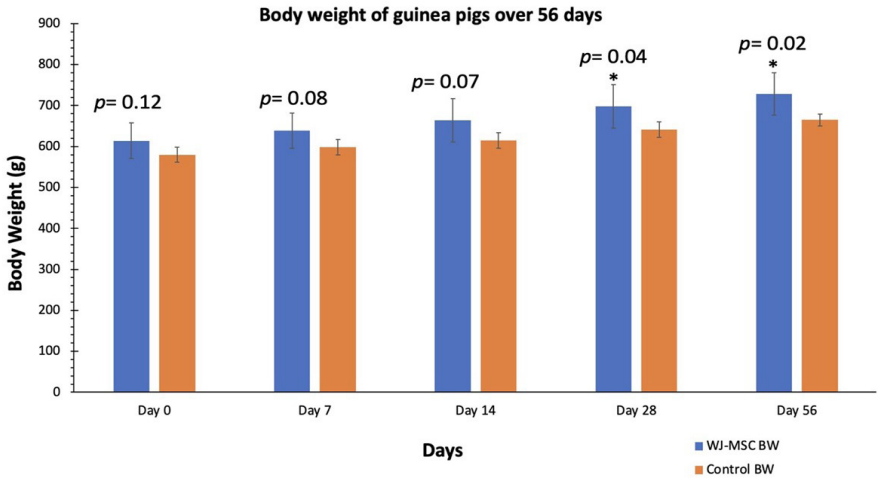

FIGURE 3: Comparison of the body weight of guinea pigs at day 0, 7, 14, 28 and 56. Guinea pigs in the WJ-MSC-treated groups exhibited higher body weights compared to the control group over the 56 days, with significant increases in body weight observed at days 28 and 56 of the experiment. Data were presented as mean ± standard deviation. $p < 0.05$* was considered significant. WJ-MSC group sample size: 6, Control group sample size: 4. *p*-values via independent sample test, SPSS on day 0: 0.12, Day 7: 0.08, Day 14: 0.07, Day 28: 0.04*, Day 56: 0.02*. Body weight represented as average ± standard deviation .

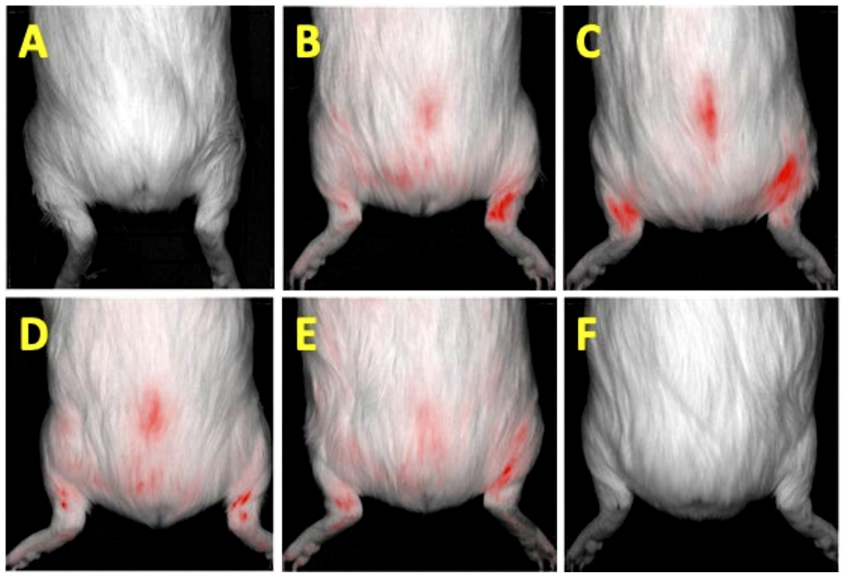

FIGURE 4: Tracking the presence of the labeled WJ-MSCs with PKH26 fluorescent dye after intra-articular injection of cells in guinea pigs using IVIS Lumina III imaging. (A) No fluorescent signal was detected before WJ-MSC injection on day 0; (B) A high-intensity fluorescent signal was detected on the right hind knee on day 0 immediately after knee intra-articular injection with WJ-MSCs; (C) On day 7, there was a fluorescent signal from the bilateral knee and caudal region of the guinea pig's body, which could correspond to the guinea pig's spine. Similar signal patterns are seen on day 14 (D) and day 28 (E). On day 56 (F), no more fluorescent signals were detected during the imaging procedure. Assumption of injected WJ-MSCs had been eliminated from the guinea pig body by day 56.

exhibited rough cartilage surfaces with evident deep erosions on both the femoral condyle and tibial plateau (Figure 5B). Osteoarthritic changes were most pronounced at the medial tibial plateau.

Osteoarthritis Research Society International Cartilage Scoring

To assess the severity of cartilage damage in the animals, the OARSI cartilage scoring system was used. The average joint score of the WJ-MSC-treated group was 3.5, and the control group was 9.0. The WJ-MSC-treated group had a lower joint score, indicating there was improvement of the joint cartilage post-WJ-MSC injection. Table 5 summarised the macroscopic evaluation of cartilage damage in the knee joints of guinea pigs following intra-articular intervention. Lesions were assessed at two anatomical locations: the femur condyle and tibia plateau. For each site, both the severity (grade) and the area affected were recorded, and a joint score was calculated by multiplying these values (Grade × Area) (Rutgers et al. 2010). The total joint score for each guinea pig reflected the cumulative damage across both regions. Higher scores indicated more severe cartilage injury. This scoring system provided a quantitative comparison of joint integrity across the study subjects.

Histology Examination and Cartilage Thickness Measurement

Histological evaluation of guinea pig knee joints revealed notable differences between the WJ-MSC-treated and control groups. H&E-stained sections (Figure 6A) from the WJ-MSC group showed more organised cartilage architecture with intact joint surfaces, while the control group exhibited signs of cartilage erosion and disorganisation. Safranin O staining further confirmed these observations, with stronger red staining in the WJ-MSC group indicating higher proteoglycan retention in the cartilage matrix. In contrast, the control group demonstrated reduced staining intensity, suggesting cartilage degradation. These findings supported the

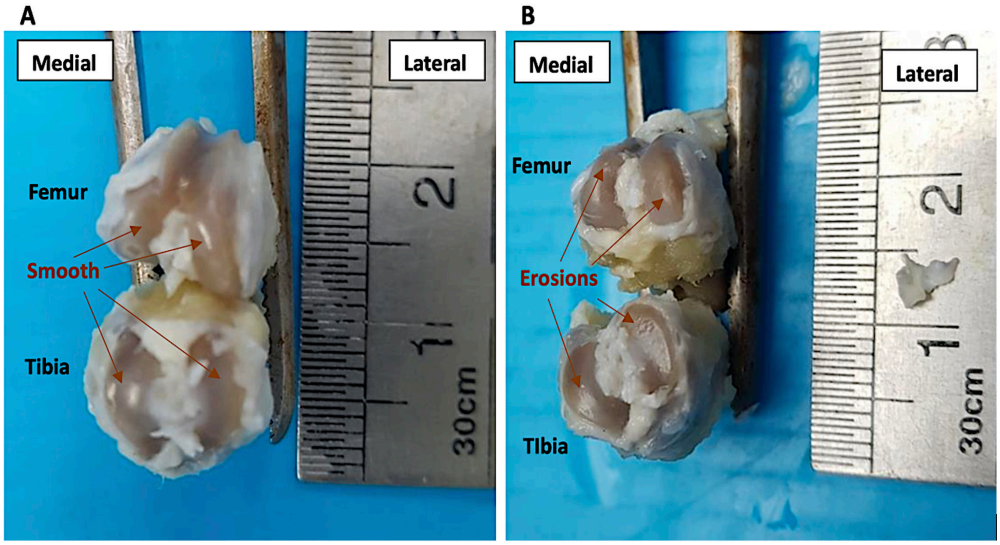

FIGURE 5: Macroscopic examination of harvested knees from the WJ-MSC-treated group and the control group. (A) Knee joint post-intra-articular WJ-MSC injection. The femur condyles (top) and the tibial plateau (bottom) surfaces were smooth; (B) The knee joint of the control group showed deep erosions at the cartilage surface of the femur condyles (top) and tibia plateau (bottom).

TABLE 5: Macroscopic joint scoring of guinea pig knee cartilage based on lesion grade and affected surface area. Each knee joint was evaluated at the femur condyle and tibia plateau surfaces for lesion severity (grade) and lesion size (area in mm^2). The joint score was calculated by multiplying the grade by the corresponding lesion area. The total joint score represents the sum of scores from both anatomical regions for each animal. Groups 1-6 received WJ-MSC as treatment, and groups 7-10 represented the control received normal saline

Guinea pig	Grade	Area (mm2)	Joint score = Grade x Area	Total joint score
GP 1: WJ-MSCs	Femur condyle: 0 Tibia plateau: 1	Femur condyle: 0 Tibia plateau: 2	Femur condyle: 0 Tibia plateau: 2	2
GP 2: WJ-MSCs	Femur condyle: 1 Tibia plateau: 2	Femur condyle: 1 Tibia plateau: 2	Femur condyle: 1 Tibia plateau: 4	5
GP 3: WJ-MSCs	Femur condyle: 1 Tibia plateau: 1	Femur condyle: 2 Tibia plateau: 1	Femur condyle: 2 Tibia plateau: 1	3
GP 4: WJ-MSCs	Femur condyle: 1 Tibia plateau: 2	Femur condyle: 1 Tibia plateau: 2	Femur condyle: 1 Tibia plateau: 4	5
GP 5: WJ-MSCs	Femur condyle: 0 Tibia plateau: 2	Femur condyle: 0 Tibia plateau: 2	Femur condyle: 0 Tibia plateau: 4	4
GP 6: WJ-MSCs	Femur condyle: 0 Tibia plateau: 1	Femur condyle: 0 Tibia plateau: 2	Femur condyle: 0 Tibia plateau: 2	2
WJ-MSC: OARSI cartilage scoring = 3.5 ± 1.3 (Average ± SD)				
GP 7: Control	Femur condyle: 2 Tibia plateau: 2	Femur condyle: 2 Tibia plateau: 2	Femur condyle: 4 Tibia plateau: 4	8
GP 8: Control	Femur condyle: 3 Tibia plateau: 2	Femur condyle: 2 Tibia plateau: 2	Femur condyle: 6 Tibia plateau: 4	10
GP 9: Control	Femur condyle: 2 Tibia plateau: 3	Femur condyle: 2 Tibia plateau: 2	Femur condyle: 4 Tibia plateau: 6	10
GP 10: Control	Femur condyle: 2 Tibia plateau: 2	Femur condyle: 2 Tibia plateau: 2	Femur condyle: 4 Tibia plateau: 4	8

Control: OARSI cartilage scoring= 9.0 ± 1.1 (Average ± SD)
The average OARSI cartilage scoring for the WJ-MSCs group is: 21/6=3.5 < 9.0 in the control group
WJ-MSCs: Wharton's jelly-derived mesenchymal stem cells; OARSI: The Osteoarthritis Research Society International

protective effect of WJ-MSCs on joint cartilage integrity. As shown in Figure 6B, quantitative comparison of cartilage thickness across joint regions revealed a consistent increase in the WJ-MSC-treated group compared to the control group. Specifically, the medial femoral condyle showed the highest improvement, with an average thickness of 325.3 μm in WJ-MSC-treated joints versus 156.3 μm in controls. The medial tibia plateau also showed a notable increase (294.4 μm vs. 199.6 μm), followed by the lateral tibia plateau (283.6 μm vs. 195.8 μm) and lateral femoral condyle (236.8 μm vs. 173.6 μm). These measurements indicated that WJ-MSC administration effectively preserved or enhanced cartilage thickness in all anatomical regions examined, suggesting a protective or regenerative effect on the articular cartilage. Table 6 showed cartilage thickness measurements at different regions, SD and CI.

Figure 6C illustrated the tidemark (yellow arrows), marking the boundary between non-calcified and calcified cartilage, which was visible in both groups and reflects the osteoarthritic nature of the model. The WJ-MSC–treated joint shows thicker, more uniformly Safranin O–stained cartilage and a more continuous cartilage–bone interface compared with the control, where cartilage thinning and structural irregularity were more evident. The green arrow indicated a marginal osteophyte, a characteristic feature of osteoarthritis representing pathological

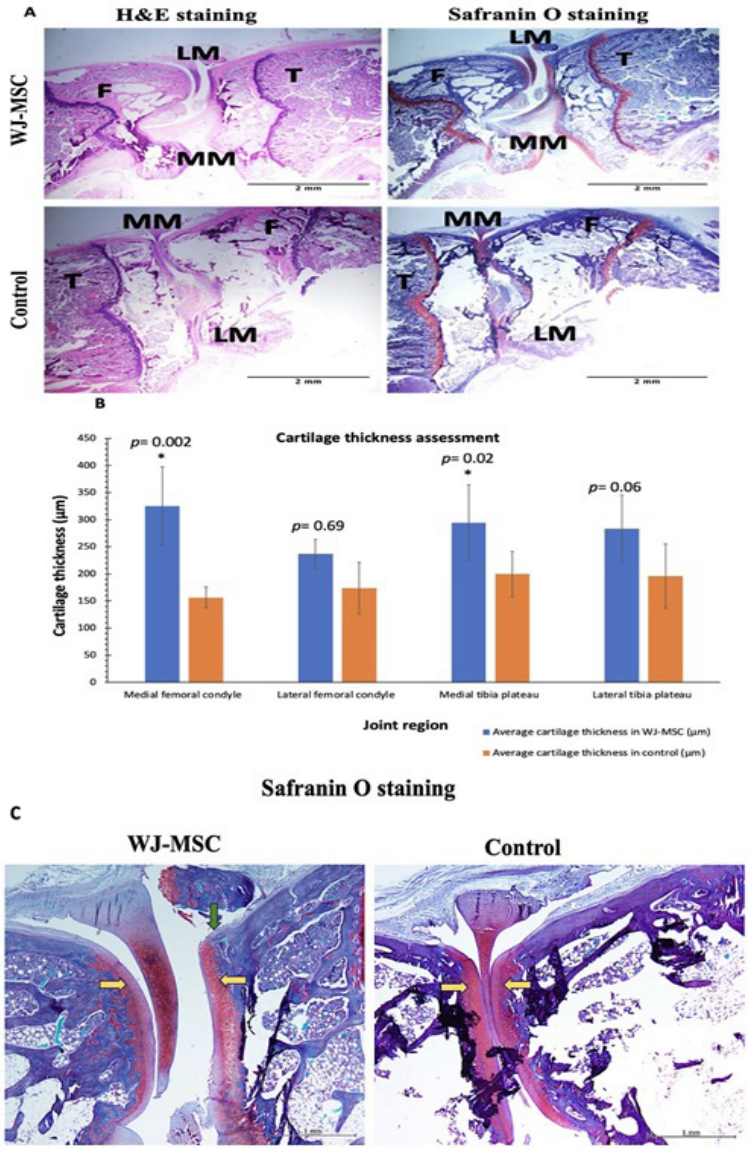

FIGURE 6: **(A) Histological comparison of articular cartilage in guinea pig knees between WJ-MSC-treated and control groups using hematoxylin and eosin (H&E) and Safranin O staining.** H&E staining (left side of the image) represented overall tissue structure, while safranin O staining (right side of the image) indicated proteoglycan content within the cartilage matrix. WJ-MSC-treated joints showed better structural integrity and more intense red staining, suggesting higher proteoglycan levels compared to the control group. Abbreviations: F: Femur; T: Tibia; MM: Medial meniscus; LM: Lateral meniscus. Scale bar of 2 mm; **(B) Quantitative assessment of cartilage thickness in the guinea pig knee across different anatomical regions.** Bar graph compared the average cartilage thickness (in µm) in the WJ-MSC-treated and control groups in the medial femoral condyle, lateral femoral condyle, medial tibia plateau and lateral tibia plateau. WJ-MSC-treated joints consistently exhibited greater cartilage thickness in all regions compared to controls, with a significantly higher cartilage thickness in the medial femoral condyle and medial tibia plateau. **(C) Safranin O staining of the guinea pig knee from the WJ-MSC-treated and control group. Yellow arrows indicate the tidemark, while the green arrow indicates osteophyte formation.** Scale bar of 1 mm $p < 0.05$* was considered significant. WJ-MSC group sample size: 6, Control group sample size: 4. p-values via independent sample test, SPSS for medial femoral condyle: 0.002*, Lateral femoral condyle: 0.69, medial tibia plateau: 0.02*, lateral tibia plateau: 0.06*, Day 56: 0.02*. Cartilage thickness represented as average ± standard deviation

bone remodeling at the joint edge. The presence of an osteophyte in the WJ-MSC–treated group reflected the underlying osteoarthritic joint environment rather than treatment success or failure. These features were shown for morphological illustration only and were not quantitatively assessed.

These results indicated a percentage increase in cartilage thickness (Table 7) in the WJ-MSCs group compared to the control group. The medial femoral condyle showed the highest increase (108%), followed by the medial tibia plateau (47%), lateral tibia plateau (45%) and lateral femoral condyle (36%), indicating region-specific responsiveness to WJ-MSC therapy.

In addition, the results of Hedges'g SPSS analysis revealed values of 2.6 for the medial femoral condyle, 1.5 for the lateral femoral condyle, 1.4 for the medial tibia plateau and 1.3 for the lateral tibia plateau for cartilage thickness. These results ranged from approximately 1.3 to 2.6 across the assessed joint regions, indicating that cartilage thickness in the WJ-MSC-treated group was 1.3-2.6 standard deviations greater than in the control group. While these findings did not constitute definitive proof of efficacy due to the exploratory nature and limited sample size of this pilot study, they indicated a biologically meaningful trend favouring WJ-MSC treatment and supported the rationale for further

TABLE 6: Cartilage thickness measurements (μm) of guinea pigs in the WJ-MSC treatment group (n = 6) and control group (n = 4) on day 56

Group	Medial femoral condyle (μm)	Lateral femoral condyle (μm)	Medial tibia plateau (μm)	Lateral tibia plateau (μm)
WJ-MSC				
Mean	325.3	236.8	294.4	283.6
SD	72.1	26.7	69.5	61.8
95% CI	249.5–401.1	208.7–264.9	221.3–367.4	218.6–348.6
Control				
Mean	156.3	173.6	199.6	195.8
SD	19.1	47.6	42.0	59.2
95% CI	125.8–186.8	97.3–249.4	132.6–266.6	101.5–290.0

SD: Standard deviation, CI: Confidence interval

TABLE 7: Percentage increase in cartilage thickness across joint regions following WJ-MSC-treated group compared to the control group. The percentage increase was calculated by comparing mean cartilage thickness in WJ-MSC-treated joints to the corresponding values in the control group for each anatomical region.

Joint Region	% Increase in WJ-MSC vs. Control
Medial femoral condyle	108%
Lateral femoral condyle	36%
Medial tibia plateau	47%
Lateral tibia plateau	45%

Formula: (Average cartilage thickness of WJ-MSCs- Average cartilage thickness of control)/(Average cartilage thickness of control))*100

WJ-MSCs: Wharton's jelly-derived mesenchymal stem cells.

adequately powered confirmatory studies.

DISCUSSION

In this study, we tracked the durability of tagged WJ-MSCs and their regenerative efficacy after intra-articular injection in guinea pigs. A single dose of 1.7×10^7 WJ-MSCs was administered, as it produced the strongest fluorescent signal in IVIS imaging following PKH26 labelling. This strong signal suggests that a higher number of viable, labelled cells remained persistent, allowing for more accurate in-vivo tracking of cell distribution and retention (Zarychta-Wiśniewska et al. 2017). Before administration of cells in the guinea pig's knee, the cells were investigated for their purity and multipotency potential via characterisation and trilineage differentiation capacity, to confirm their identity as MSCs and ensure their suitability for application in this experiment (Mallis et al. 2020; Nadeem et al. 2024). Animal general health was monitored, including their body weight measurement, throughout the study. As a result, the WJ-MSC-treated group showed numerically higher body weight than the control group, with significantly higher body weight in the WJ-MSC group on days 28 and 56. However, these differences should be regarded as observations interpreted with caution. Body weight is a multifactorial parameter and was not a primary endpoint of this study; factors such as individual metabolism, feeding behaviour, stress and environmental variations (e.g., cage conditions and handling) could have contributed to the observed pattern. Although the trend is broadly consistent with the favourable macroscopic and histological findings, the present data do not allow us to attribute body-weight changes directly to WJ-MSC treatment and further targeted studies would be required to clarify this.

In this study, in vivo imaging using PKH26-labelled WJ-MSCs showed that the injected cells localised primarily to the bilateral knees and lower spinal region from day 0 to day 28, with signal intensity gradually decreasing and fully disappearing by day 56 (Figure 4). This early and targeted localisation aligns with an increase in cartilage thickness, especially a significant increase in cartilage thickness observed in the medial femoral condyle and medial tibia plateau, as detected in histological observation (Figure 6A) and cartilage thickness measurement (Figure 6B). The presence of WJ-MSCs in the joint region during the early phase likely allowed them to exert paracrine effects or modulate the local environment, promoting cartilage preservation or regeneration. Although the cells were no longer detectable by day 56, their temporary presence in key joint areas appears to have had a lasting therapeutic impact.

Additionally, the signal detected around both knees and in the lower spine (Figure 4) indicates that some of the injected cells may have leaked out during intra-articular injection, likely due to the small size of the guinea pig knee joint. This unintended cell distribution to other regions has several implications for interpreting our findings. It suggests that not all delivered cells remained within the joint, which may highlight that the effective intra-articular dose may have been lower than intended. Furthermore, fluorescence in periarticular and caudal regions raises the possibility of imaging artifacts or superficial dye redistribution, making it difficult to determine the exact fate of the cells based on IVIS imaging alone.

Moreover, any leakage may highlight a technical limitation of intra-articular delivery in small animal models, where a small joint capsule may increase the risk of overflow compared with larger species. Although the fluorescent signals diminished over time and disappeared by day 56, indicating no long-term extra-articular retention, these findings underscore the need for improved injection precision and complementary tracking methods in future studies. A suggestion could be techniques such as ultrasound-guided injection to help better distinguish true biodistribution from procedural leakage.

As a result of macroscopic examination of the WJ-MSCs-treated knee compared to the control group (Figure 5), the smooth cartilage surfaces on the femoral condyle and tibial plateau indicate effective cartilage regeneration and repair.

This smooth surface may suggest restoration of cartilage structure integrity and function, and possibly reflect the anti-inflammatory, immunomodulatory and chondroprotective effect of WJ-MSCs. Considering that WJ-MSC treatment can promote chondrogenic differentiation, increasing production of collagen and extracellular matrix components essential for healthy cartilage (Molnar et al. 2022), suppress cartilage degradation by modulating MMPs and their inhibitors (TIMPs), followed by maintaining cartilage homeostasis and preventing further breakdown (Molnar et al. 2022), and create a regenerative microenvironment through secretion of bioactive factors that reduce inflammation and stimulate endogenous repair mechanisms (Baghaban Eslaminejad & Malakooty Poor 2014), raise the idea that WJ-MSC therapy could successfully mitigate cartilage damage, promote regeneration of cartilage and restore joint surface smoothness, which is critical for normal joint function and pain reduction. This interpretation aligns with findings from multiple studies, showing that MSCs, including WJ-MSCs, contribute to cartilage repair by enhancing matrix synthesis, reducing catabolic enzyme activity and improving cartilage morphology (Baghaban Eslaminejad & Malakooty Poor 2014; Le et al. 2020; Molnar et al. 2022).

To investigate further the severity of cartilage damage, the OARSI cartilage score was measured (Table 5) for both the WJ-MSC and the control groups. An OARSI cartilage score of 3.5 in the WJ-MSC treated group compared to a score of 9 in the control group indicates a substantially lower severity of cartilage degeneration in the treated group. Since OARSI scoring combines grades (depth of cartilage damage) and stage (extent of cartilage surface affected), a lower score reflects less cartilage erosion, better preservation of cartilage structure and milder OA changes. This suggests that WJ-MSC treatment effectively mitigated cartilage damage and promoted repair, resulting in improved cartilage integrity and function compared to the control group, which shows advanced degeneration with a high OARSI score. Such a difference aligns with findings that higher OARSI grades correlate with decreased cartilage stiffness and function (Ashinsky et al. 2015; Waldstein et al. 2016), so a score reduction from 9 to 3.5 represents meaningful cartilage protection and regeneration in response to WJ-MSC treatment.

To histologically assess the results of this investigation, H&E-stained sections (Figure 6A) showed more organised cartilage architecture in the WJ-MSC-treated group in comparison to the control group. This means that the cartilage tissue in the WJ-MSC group maintained a healthier, well-structured arrangement of cells and extracellular matrix, with a smooth and continuous joint surface indicative of effective cartilage repair or protection. In contrast, the control group showed disrupted cartilage structure, with visible erosion and loss of normal tissue organisation, reflecting ongoing cartilage degradation typical of OA.

Further investigation using Safranin O staining, specifically stained proteoglycans, which are critical components of cartilage matrix that provide strength and elasticity (Moussa et al. 2024). The stronger red staining in the WJ-MSC group in response to Safranin O staining indicates that these treated joints retained more proteoglycans, suggesting better preservation or regeneration of the cartilage matrix. This supports the idea that WJ-MSC therapy helps maintain the biochemical integrity of cartilage, which is essential for its function.

The results of the quantitative cartilage thickness measurement (Figure 6B), with significantly higher cartilage thickness in the WJ-MSC-treated group in the medial femoral condyle and medial tibia plateau, demonstrate that WJ-MSC either preserved existing cartilage or stimulated new cartilage growth. Since cartilage thinning is a hallmark of OA progression (Gupta et al. 2004), this result may indicate a protective or regenerative effect of WJ-MSC on the articular cartilage, improving joint health across multiple key load-bearing regions. This suggestion is aligned with previously published preclinical studies where WJ-MSC therapy demonstrated greater chondrogenic and regenerative potential than some other MSC sources, attributed to their

high proliferation, immunomodulatory capacity and secretome richness (Lam et al. 2020).

On the clinical side, an open-label phase I/II study reported that repeated intra-articular injections of WJ-MSCs in knee OA were well tolerated and associated with improved pain, function, and MRI evidence of cartilage repair at 1-year follow-up (Ao et al. 2023). Moreover, a recent meta-analysis of MSC therapies for OA found meaningful clinical improvements at 12 months post-injection, especially with lower cell doses, highlighting the importance of dose optimisation (Rahmadian et al. 2025).

In this context, our guinea-pig OA model using intra-articular WJ-MSC injections adds relevant data: unlike many prior works focusing on symptomatic relief or short-term follow-up, our study provides cartilage structural outcomes (thickness, histology, macroscopic scoring) alongside cell-tracking data. This may contribute to bridging a critical gap between symptomatic human trials and mechanistic pre-clinical work by suggesting WJ-MSC therapy may offer true regenerative benefits, not just symptomatic relief. At the same time, our data underscores remaining uncertainties, especially persistence time and cell retention, reinforcing the need for further dose-response studies and longer-term pre-clinical-to-clinic translation.

In our results, the findings that WJ-MSC treatment statistically increased a significant cartilage thickness only in the medial femoral condyle and medial tibia plateau suggest several important points as outlined below.

The medial femoral condyle and medial tibia plateau are commonly affected regions in the knee in OA patients (Azari et al. 2024). Therefore, these regions may experience greater mechanical stress and cartilage wear, making them more responsive to regenerative treatments like WJ-MSCs. Hence, the significant increase in cartilage thickness in these regions may indicate that WJ-MSC may be particularly effective in areas with more pronounced degeneration or where the microenvironment is more conducive to cartilage repair. Moreover, even though cartilage thickness increased in all knee regions after WJ-MSC treatment, only some increases reached a level of statistical significance. Whether an increase is statistically significant depends on how large the change is, how consistent the results are across different groups, and how many animals were studied.

In the lateral femoral condyle and lateral tibia plateau, the increases might have been smaller or more inconsistent between the animals, or these areas might have had less cartilage damage to begin with, making it harder to detect a clear, statistically significant improvement. This does not mean the treatment did not help these regions at all; rather, the data more strongly support a clear benefit in the medial regions where changes were larger and more consistent (Erb 1990; Kyonka 2018). Therefore, the limited number of animals used in this preliminary investigation may not allow us to detect statistically meaningful differences. However, this study was ethically approved to perform the primary investigation for future research.

The structural improvements observed in the WJ-MSC group, such as increased cartilage thickness, better histology and lower OARSI score, are consistent with the known paracrine action of WJ-MSCs in OA. WJ-MSCs are rich in anti-inflammatory mediators that can reduce synovial inflammation, therefore helping preserve cartilage. At the same time, growth factors released by WJ-MSCs support chondrocyte survival and stimulate extracellular matrix (ECM) regeneration (Barlian et al. 2020), which aligns with the restoration of cartilage seen in histology results. The combined anti-inflammatory and regenerative signaling profile of WJ-MSCs provides a plausible mechanistic explanation for the protective and reparative effects demonstrated in this study.

This study has several limitations. The overall sample size was small, reflecting the exploratory nature of the work and ethical considerations to minimise animal use. We acknowledge that the small sample size and absence of a power analysis are major limitations that reduce statistical strength and increase the risk of false-positive findings. However, this study was designed as

a preliminary proof-of-concept to justify larger experiments. Future work will include power calculation and parameters to validate these early observations.

Although three doses were initially screened during preliminary IVIS testing, only a single intra-articular dose was carried forward in the main experiment to reduce animal numbers and because the high dose provided the most reliable fluorescent signal for tracking purposes. Functional assessments such as gait or weight-bearing tests were not included, as the primary objective was to evaluate structural changes and track cell persistence; nevertheless, future studies would benefit from incorporating behavioral outcomes.

Moreover, the missed imaging at day 42 was an unavoidable consequence of COVID-19 movement restrictions at the time. The missed imaging on day 42 introduces some uncertainty regarding the exact timing of signal disappearance, as we cannot determine whether the fluorescent signal was still present on day 42 or had already declined to undetectable levels before day 56. Despite this gap, the available data at days 0, 7, 14 and 28 show a progressive reduction in signal intensity, indicating a consistent clearance trend. The absence of detectable fluorescence at day 56 confirms that the cells were eliminated by that time, although the precise point of disappearance cannot be pinpointed. We acknowledge that this missing datapoint reduces temporal precision, and future studies incorporating uninterrupted imaging schedules will allow a clearer understanding of intermediate clearance dynamics.

The follow-up period of 56 days offered insight into short-term effects but is insufficient to fully assess long-term safety, including ectopic tissue formation, prolonged cell persistence or tumorigenic risk. Another limitation is the use of a xenograft model, as human WJ-MSCs were injected into guinea pigs; cross-species differences in immune response and joint biology may influence cell behaviour and therapeutic potential. However, xenografting is widely used in early-stage research and WJ-MSCs exhibit low immunogenicity (Drobiova et al. 2023), enabling short-term safety and mechanistic evaluation before progressing to species-matched or large-animal models. Additionally, PKH26 labeling carries the known possibility of dye transfer to host cells or extracellular retention, which may confound biodistribution interpretation. Despite these limitations, the findings provide valuable proof-of-concept data to guide the design of more comprehensive future studies.

CONCLUSION

In conclusion, this exploratory proof-of-concept study provides a base for future investigations using WJ-MSCs for OA with preliminary evidence supporting the potential of WJ-MSCs as a therapeutic option. In our Dunkin Hartley guinea pigs model, WJ-MSC administration was associated with favourable structural changes, including lower OARSI score and improved cartilage appearance without observed signs of malignancy. The disappearance of fluorescent signals by day 56 suggests short-term safety; however, this timeframe is insufficient to rule out late-onset safety concerns such as ectopic tissue formation, long-term cell persistence, or tumorigenic risk. Therefore, extended longitudinal studies are essential to confirm safety and durability. Importantly, these results were obtained in an animal model and should not be directly translated to human clinical outcomes. Overall, findings of this study should be interpreted as early proof-of-concept rather than definitive evidence of efficacy, and further research including a larger sample size, dose-response evaluation, functional outcome assessments and extended follow-up, is required to clarify the therapeutic potential of human WJ-MSCs in the treatment of degenerative knee OA. The extensive WJ-MSC characterisation data were included to ensure transparency, reproducibility, and compliance with MSC identity and quality standards, which are essential prerequisites for any preclinical study involving human-derived cell products.

Author contributions: Clinical-grade testing of WJ-MSC: KC, PK, RS, RR; Conducted the lab experiments: AFMD, NM, SY; Data analysis: SK; Writing-original draft and writing-review and editing: SK; Surpervision: BAHY

Funding: This research was supported by Fundamental Grant of Faculty of Medicine, UKM (Project Code: FF-2019-460).
Acknowledgment: The authors want to thank the Department of Orthopedic & Traumatology and the Faculty of Medicine, UKM, for providing them with access to the facilities necessary to complete this research experiment.

Conflict of interest: The authors of this manuscript declare no conflict of interest.

Ethics statement: The animal ethics for this study was approved by the UKM Animal Ethics Committee (PPUKM/2019/BADRUL AKMAL/25-SEPT/1038-OCT-2019-MARCH-2020) on 24 October 2019.

REFERENCES

Animal Research Review Panel. 2023. Animal research review panel guidelines for the housing of guinea pigs in scientific institutions. *Department of Regional NSW*. https://www.dpi.nsw.gov.au/__data/assets/pdf_file/0012/222510/x10.2.2-Guideline-21-ARRP-Guidelines-for-the-Housing-of-Guinea-Pigs-in-Scientific-Institutions.pdf (Accessed on October 2025).

Ao, Y., Duan, J., Xiong, N., Qian, N., Zhang, R., Yang, L., Yu, S., Wang, F. 2023. Repeated intra-articular injections of umbilical cord-derived mesenchymal stem cells for knee osteoarthritis: A phase I, single-arm study. *BMC Musculoskeletal Disord* **24**(1): 488. https://doi.org/10.1186/s12891-023-06555-y.

Aratikatla, A., Maffulli, N., Gupta, M., Potti, I.A., Potty, A.G., Gupta, A. 2024. Wharton's Jelly and osteoarthritis of the knee. *Br Med Bull* **149**(1): 13-31. https://doi.org/10.1093/bmb/ldad030.

Ashinsky, B.G., Coletta, C.E., Bouhrara, M., Lukas, V.A., Boyle, J.M., Reiter, D.A., Neu, CP., Goldberg, I.G., Spencer, R.G. 2015. Machine learning classification of OARSI-scored human articular cartilage using magnetic resonance imaging. *Osteoarthritis Cartilage* **23**(10): 1704-12. https://doi.org/10.1016/j.joca.2015.05.028.

Azari, F., Colyn, W., Bellemans, J., Scheys, L., Harry van Lenthe, G. 2024. Correlation between tibial and femoral bone and cartilage changes in end-stage knee osteoarthritis. *JBMR Plus* **8**(4): ziae014. https://doi.org/10.1093/jbmrpl/ziae014

Baghaban Eslaminejad, M., Malakooty Poor, E. 2014. Mesenchymal stem cells as a potent cell source for articular cartilage regeneration. *World J Stem Cells* **6**(3): 344-54. https://doi.org/10.4252/wjsc.v6.i3.344

Barlian, A., Judawisastra, H., Ridwan, A., Wahyuni, A.R., Lingga, M.E. 2020. Chondrogenic differentiation of Wharton's Jelly mesenchymal stem cells on silk spidroin-fibroin mix scaffold supplemented with L-ascorbic acid and platelet rich plasma. *Sci Rep* **10**(1): 19449. https://doi.org/10.1038/s41598-020-764.

Česnik, A.B., Švajger, U. 2024. The issue of heterogeneity of MSC-based advanced therapy medicinal products - A review. *Front Cell Dev Biol* **26**(12): 1400347. https://doi.org/10.3389/fcell.2024.1400347

Cheng, W.D., Bin, L., Lin, Z. X., Yu, D., Xiang, D. K., Lo, S., Ravichandran, M., Kong, T. S. 2024. Human umbilical cord mesenchymal stem cells toxicity and allergy effects: In vivo assessment. *PLOS ONE* **19**(10): e0309429. https://doi.org/10.1371/journal.pone.0309429.

Crescencia, A. 2024. Clinical Trials and regulatory challenges in mesenchymal stem cell Therapy. *J Mol Hist Med Phys* **9**(3). https://doi.org/10.37421/2684-494X.2024.9.230

Drobiova, H., Sindhu, S., Ahmad, R., Haddad, D., Al-Mulla, F., Al Madhoun, A. 2023. Wharton's Jelly mesenchymal stem cells: A concise review of their secretome and prospective clinical applications. *Front Cell Dev Biol* **27**(11): 1211217. https://doi.org/10.3389/fcell.2023.1211217

Endrinaldi, E., Darwin, E., Zubir, N., Revilla, G. 2019a. The effect of mesenchymal stem cell Wharton's Jelly on ADAMTS-4 and iNOS levels in osteoarthritis rat model. *Open Access Maced J Med Sci* **7**(8): 1270-5. https://doi.org/10.3889/oamjms.2019.155

Endrinaldi, E., Darwin, E., Zubir, N., Revilla, G. 2019b. The effect of mesenchymal stem cell Wharton's Jelly on matrix metalloproteinase-1 and interleukin-4 levels in osteoarthritis rat model. *Open Access Maced J Med Sci* **7**(4): 529-35. https://doi.org/10.3889/oamjms.2019.152

Erb, H.N. 1990. A statistical approach for calculating the minimum number of animals needed in research. *ILAR News* **32**(1): 11-6. https://doi.org/10.1093/ilar.32.1.11.

Ghamrawi, A., Basso, R., Shakik, N., Haddad, L., Nasr, Z., Harmouch, C. 2025. Wharton's Jelly mesenchymal stem cells: Shaping the future of osteoarthritis therapy with advancements in

chitosan-hyaluronic acid scaffolds. *Stem Cells Dev* **34**(102): 1-16. https://doi.org/10.1089/scd.2024.0033.

Goldring, M.B. 2012. Articular cartilage degradation in osteoarthritis. *HSS J* **8**(1): 7-9. https://doi.org/10.1007/s11420-011-9250-z

Goto, T., Murata, M., Nishida, T., Terakura, S., Kamoshita, S., Ishikawa, Y., Ushijima, Y., Adachi, Y., Suzuki, S., Kato, K., Hirakawa, A., Nishiwaki, S., Nishio, N., Takahashi, Y., Kodera, Y., Matsushita, T., Kiyoi, H. 2021. Phase I clinical trial of intra-bone marrow cotransplantation of mesenchymal stem cells in cord blood transplantation. *Stem Cells Transl Med* **10**(4): 542-553. https://doi.org/10.1002/sctm.20-0381.

Gupta, K.B., Duryea, J., Weissman, B.N. 2004. Radiographic evaluation of osteoarthritis. *Radio Clin North Am* **42**(1): 11-41. https://doi.org/10.1016/S0033-8389(03)00169-6.

Harrell, C.R., Markovic, B.S., Fellabaum, C., Arsenijevic, A., Volarevic, V. 2019. Mesenchymal stem cell-based therapy of osteoarthritis: Current knowledge and future perspectives. *Biomed Pharmacother* **109**: 2318-26. https://doi.org/10.1016/j.biopha.2018.11.099.

Horie, M., Choi, H., Lee, R.H., Reger, R.L., Ylostalo, J., Muneta, T., Sekiya, I., Prockop, D.J. 2012. Intra-articular Injection of human mesenchymal stem cells (MSCs) promote rat meniscal regeneration by being activated to express indian hedgehog that enhances expression of type II Collagen. *Osteoarthritis* **20**(10): 1197-207. https://doi.org/10.1016/j.joca.2012.06.002.

Kent State University Libraries. 2025. Independent Samples t Test - SPSS Tutorials – LibGuides. https://libguides.library.kent.edu/spss/independentttest [Accessed on 20 January 2026].

Jiang, P., Hu, K., Jin, L., Luo, Z. 2024. A brief review of current treatment options for osteoarthritis including disease-modifying osteoarthritis drugs (DMOADs) and novel therapeutics. *Ann Med Surg* **86**(7): 4042-8. https://doi.org/10.1097/MS9.0000000000002214.

Kyonka, E.G.E. 2018. Tutorial: Small-N Power Analysis. *Perspect Behav Sci* **42**(1): 133.

Lam, A.T.L., Reuveny, S., Oh, S.K.W. 2020. Human mesenchymal stem cell therapy for cartilage repair: Review on isolation, expansion, and constructs. *Stem Cell Res* **44**: 101738. https://doi.org/10.1016/j.scr.2020.101738.

Le, H., Xu, W., Zhuang, X., Chang, F., Wang, Y., Ding, J. 2020. Mesenchymal stem cells for cartilage regeneration. *J Tissue Eng* **11**: 2041731420943839. https://doi.org/10.1177/2041731420943

Li, P., Zhang, R., Sun, H., Chen, L., Liu, F., Yao, C., Du, M., Jiang, X. 2012. PKH26 can transfer to host cells in vitro and vivo. *Stem Cells Deve* **22**(2): 340-44. https://doi.org/10.1089/scd.2012.0357.

Liang, H., Suo, H., Wang, Z., Feng, W. 2020. Progress in the treatment of osteoarthritis with umbilical cord stem cells. *Hum Cell* **33**(3): 470-5. https://doi.org/10.1007/s13577-020-00377-z.

Luo, X., Shen, X., Kang, R., Huang, W., Zhu, Z., Liao, J. 2025. A cross-sectional study unveiling the global impact and future projections through 2060 of osteoarthritis. *Eur J Public Health* **23**: ckaf087. https://doi.org/10.1093/eurpub/ckaf087.

Mallis, P., Papapanagiotou, A., Katsimpoulas, M., Kostakis, A., Siasos, G., Kassi, E., Stavropoulos-Giokas, C., Michalopoulos, E. 2020. Efficient differentiation of vascular smooth muscle cells from Wharton's Jelly mesenchymal stromal cells using human platelet lysate: A potential cell source for small blood vessel engineering. *World J Stem Cells* 2020; **12**(3): 203-21. https://doi.org/10.4252/wjsc.v12.i3.203

Mastrolia, I., Foppiani, E.M., Murgia, A., Candini, O., Samarelli, A.V., Grisendi, G., Veronesi, E., Horwitz, E. M., Dominici, M. 2019. Challenges in clinical development of mesenchymal stromal/stem cells: Concise review. *Stem Cells Transl Med* **8**(11): 1135-48. https://doi.org/10.1002/sctm.19-0044.

Md Yusoff, B.A.H., Mohd Don, A.F., Mohamad, N., Saravanamuthu, R., Chandran, K., Rasib, R., Kathivaloo, P., Lau, F., Yih, H. 2023. Chondrogen™ injection for knee osteoarthritis using stem cells from Wharton's Jelly. *Sains Malaysiana* **52**(10): 2773–84. http://doi.org/10.17576/jsm-2023-5210-04

Mello, D.B., Mesquita, F.C.P., Silva dos Santos, D., Asensi, K.D., Dias, M.L., Campos de Carvalho, A.C., Goldenberg, R.C. dos S., Kasai-Brunswick, T.H. 2024. Mesenchymal Stromal Cell-Based Products: Challenges and Clinical Therapeutic Options. *Int J Mol Sci* **25**(11): 6063. https://doi.org/10.3390/ijms25116063.

Molnar, V., Paveli , E., Vrdoljak, K., Čemerin, M., Klarić, E., Matiši , V., Bjelica, R., Brlek, P., Kovačić, I., Tremolada, C., Primorac, D. 2022. Mesenchymal stem cell mechanisms of action and clinical effects in osteoarthritis: A narrative review. *Genes* **13**(6): 949. https://doi.org/10.3390/genes13060949.

Moussa, S.A.E.D.M., Zaki, M.G.E.D., Mohamed, M.O., Abo Zeid, A.A., Farrag, D.A. 2024. Efficacy of adipose—derived stromal vascular fraction in treatment of osteoarthritis: an experimental study. *Egypt Rheumatol Rehabil* **51**(1): 1-11. https://doi.org/10.1186/s43166-024-00250-z.

Musci, R.V., Walsh, M.A., Konopka, A.R., Wolff, C.A., Peelor, F.F., Reiser, R.F., Santangelo, K.S., Hamilton, K.L. 2020. The dunkin hartley guinea pig is a model of primary osteoarthritis that also

exhibits early onset myofiber remodeling that resembles human musculoskeletal aging. *Front Physiol* **11**: 571372. https://doi.org/10.3389/fphys.2020.571372.

Nadeem, G., Theerakittayakorn, K., Somredngan, S., Thi Nguyen, H., Boonthai, T., Samruan, W., Tangkanjanavelukul, P., Parnpai, R. 2024. Induction of human Wharton's Jelly of umbilical cord derived mesenchymal stem cells to be chondrocytes and transplantation in guinea pig model with spontaneous osteoarthritis. *Int J Mol Sci* **25**(11): 5673. https://doi.org/10.3390/ijms25115673.

Rahmadian, R., Ariliusra, Z., Kusuma, K. R. A., Ali, H., Raymond, B., Meksiko, R. 2025. Efficacy of a single intra-articular injection of mesenchymal stem cells for knee osteoarthritis: a dose-focused meta-analysis of randomized controlled trials. *J Orthop Surg Res* **20**(1): 812. https://doi.org/10.1186/s13018-025-06190-4.

Resnik, D.B., Miller, F. 2010. The ethics of sham surgery on research subjects with cognitive impairments that affect decision-making capacity. *Contemp Clin Trials* **31**(5): 407-10. https://doi.org/10.1016/j.cct.2010.05.009

Rutgers, M., Pelt, V.M.J.P., Dhert, W.J.A., Creemers, L.B., Saris, D.B.F. 2010. Evaluation of histological scoring systems for tissue-engineered, repaired and osteoarthritic cartilage. *Osteoarthr Cart* **18**(1): 12-23. https://doi.org/10.1016/j.joca.2009.08.009.

Schram, B., Orr, R., Pope, R., Canetti, E., Knapik, J. 2020. Risk factors for development of lower limb osteoarthritis in physically demanding occupations: A narrative umbrella review. *J Occup Health* **62**(1): e12103. https://doi.org/10.1002/1348-9585.12103.

Sen, R., Hurley, J. A. 2023. Osteoarthritis. In *StatPearls* Treasure Island (FL): StatPearls Publishing https://www.ncbi.nlm.nih.gov/books/NBK482326/ [Accessed on 27 July 2026]

Shin, H.S., Thakore, A., Tada, Y., Pedroza, A.J., Ikeda, G., Chen, I.Y., Chan, D., Jaatinen, K.J., Yajima, S., Pfrender, E.M., Kawamura, M., Yang, P.C., Wu, J.C., Appel, E.A., Fischbein, M.P., Woo, Y. Shudo, Y. 2022. Angiogenic stem cell delivery platform to augment post-infarction neovasculature and reverse ventricular remodeling. *Sci Rep* **12**(1): 17605. https://doi.org/10.1038/s41598-022-21510-y.

Steinmetz, J.D., Culbreth, G.T., Haile, L.M., Rafferty, Q., Lo, J., Fukutaki, K.G., Cruz, J.A., Smith, A.E., Vollset, S.E., Brooks, P.M., Cross, M., Woolf, A.D., Hagins, H., Abbasi-Kangevari, M., Abedi, A., Ackerman, I.N., Amu, H., Antony, B., Arabloo, J., Kopec, J.A. 2023. Global, regional, and national burden of osteoarthritis, 1990-2020 and projections to 2050: A systematic analysis for the Global Burden of Disease Study 2021. *Lancet Rheumatol* **5**(9): e508-22. https://doi.org/10.1016/S2665-9913(23)00163-7.

UKM. 2025. General - UKM Animal Ethical Committee (UKMAEC). UKM Animal Ethical Committee. https://www.ukm.my/ukmaec/guideline/introduction/ (Accessed on 12 December 2025).

Varaa, N., Azandeh, S., Khodabandeh, Z., Gharravi, A.M. 2019. Wharton's Jelly mesenchymal stem cell: Various protocols for isolation and differentiation of hepatocyte-like cells; Narrative review. *Iran J Med Sci* **44**(6): 437. https://doi.org/10.30476/ijms.2019.44952.

Waldstein, W., Perino, G., Gilbert, S.L., Maher, S.A., Windhager, R., Boettner, F. 2016. OARSI osteoarthritis cartilage histopathology assessment system: A biomechanical evaluation in the human knee. *J Orthop Res* **34**(1): 135-40. https://doi.org/10.1002/jor.23010.

Watson, N., Divers, R., Kedar, R., Mehindru, A., Mehindru, A., Borlongan, M. C., Borlongan, C. V. 2015. Discarded Wharton jelly of the human umbilical cord: a viable source for mesenchymal stromal cells. *Cytotherapy* **17**(1): 18-24. https://doi.org/10.1016/j.jcyt.2014.08.009.

Wellington, D., Mikaelian, I., Singer, L. 2013. Comparison of ketamine–xylazine and ketamine–dexmedetomidine anesthesia and intraperitoneal tolerance in rats. *J Am Assoc Lab Anim Sci* **52**(4): 481-7.

Wu, K.C., Chang, Y.H., Ding, D.C., Lin, S.Z. 2024. Mesenchymal stromal cells aging cartilage regeneration: A review. *Int J Mol Sci* **25**(23): 12911. https://doi.org/10.3390/ijms252312911.

Xu, J.X., Xu, F.Z., Furbish, A., Peterson, Y.K., Woster, P.M., Braxton, A.M. 2024. Micro-computed tomography analysis of the knee in aged dunkin-hartley guinea pigs after intra articular injection. *J Vis Exp* **210**: e66053. https://doi.org/10.3791/66053.

Zarychta-Wi niewska, W., Burdzinska, A., Zagozdzon, R., Dybowski, B., Butrym, M., Gajewski, Z., Paczek, L. 2017. In vivo imaging system for explants analysis-A new approach for assessment of cell transplantation effects in large animal models. *PLOS One* **12**(9): e0184588. https://doi.org/10.1371/journal.pone.0184588.

Zhang, Q., Xiang, E., Rao, W., Zhang, Y.Q., Xiao, C.H., Li, C.Y., Han, B., Wu, D. 2021. Intra-articular injection of human umbilical cord mesenchymal stem cells ameliorates monosodium iodoacetate-induced osteoarthritis in rats by inhibiting cartilage degradation and inflammation. *Bone Joint Res* **10**(3): 226-36. https://doi.org/10.1302/2046-3758.103.BJR-2020-0206.R2.

Zhou, J., Zhang, Y., Xie, S., Li, Y., Sun, Q., Tang, X., Zhao, T., Chen, X. 2025. The escalating burden of osteoarthritis in East and Southeast Asia: an information-analytical study from the GBD 2021. *Clin Rheumatol* **44**(12): 4819-32. https://doi.org/10.1007/s10067-025-07740-1.

Zhou, T., Yuan, Z., Weng, J., Pei, D., Du, X., He, C., Lai, P. 2021. Challenges and advances in clinical applications of mesenchymal stromal cells. *J Hematol Oncol* **14**(1): 24. https://doi.org/10.1186/s13045-021-01037-x.